BOREAS An international journal of Quaternary research

Sediment sequence at Muhos, western Finland – a window to the Pleistocene history of the Scandinavian Ice Sheet

TIINA ESKOLA AND JUHA P. LUNKKA

BOREAS

Eskola, T. & Lunkka, J. P. 2022 (April): Sediment sequence at Muhos, western Finland – a window to the Pleistocene history of the Scandinavian Ice Sheet. *Boreas*, Vol. 51, pp. 332–349. https://doi.org/10.1111/bor.12560. ISSN 0300-9483.

In this study, we analysed a ~54-m sediment core consisting of Quaternary sediments overlying the Neoproterozoic Muhos Formation in central western Finland, adjacent to the Gulf of Bothnia. The sediments recovered were logged, and their sedimentological characteristics defined. Two fine-grained sediment units were subjected to biostratigraphical studies using pollen and diatom analyses. In addition, two sand-rich units and a wooden stick were dated by the optically stimulated luminescence (OSL) and ^{14}C-AMS methods. The core sediments were divided into six units, where several diamicton, sand and gravel, and silt-and-clay-dominated beds were studied. The results indicate that the sediment succession of the core beneath the Holocene Litorina Sea and the Ancylus Lake sediments of the Baltic Basin were deposited in glacial and lacustrine environments that existed in the Oulu River valley during the time period between the Saalian glaciation (MIS 6) and the Holocene. The stratigraphical evidence, supported by the OSL ages, suggests that the Scandinavian Ice Sheet (SIS) entered the Muhos area during the Saalian glaciation, and at least during three separate time intervals in the Weichselian stage. Stratigraphically controlled and age-bracketed evidence shows that the first Weichselian SIS advance extended further south in the eastern part of Fennoscandia than previously estimated, and that this ice growth phase occurred during the Early Weichselian Herning Stadial (MIS 5d). The subsequent ice growth phases occurred during the Middle (MIS 4) and Late (MIS 2) Weichselian substages. The lacustrine and littoral sediments of the Muhos core were correlated with the late Eemian interglacial (MIS 5e) and two Weichselian interstadials (MIS 5c and MIS 3).

Tiina Eskola (tiina.eskola@oulu.fi) and Juha Pekka Lunkka, Geology Research Group, Oulu Mining School, University of Oulu, P.O. Box 3000, Oulu FI-90014, Finland; *received 20th January 2021, accepted 5th September 2021.*

The eastern part of Fennoscandia (Fig. 1) was covered by the Scandinavian Ice Sheet (SIS) several times during the Middle and Late Pleistocene (Saarnisto & Lunkka 2004; Svendsen *et al.* 2004; Johansson *et al.* 2011; Hughes *et al.* 2016). However, the exact number and timing of the SIS growth phases from the ice dome areas in the Scandinavian Mountains across Finland to northwestern Russia are not precisely known.

The most comprehensive study on the Pleistocene stratigraphy of northern Finland (i.e. Finnish Lapland) was conducted by Hirvas (1991). The study identified six stratigraphically significant till units overlying the Precambrian bedrock, thereby indicating six SIS growth phases across the area. Indeed, there are several sites in Finnish Lapland where till units are interbedded with sorted sands, gravels, organic-rich silt, clay/gyttja, and/or peat (Korpela 1969; Hirvas 1991; Saarnisto *et al.* 1999; Helmens *et al.* 2000; Mäkinen 2005; Lunkka *et al.* 2014; Salonen *et al.* 2014; Sarala *et al.* 2016). However, at several sites, only partial sedimentary sections or core materials have been preserved owing to erosion and glaciotectonic deformation during different glacial growth phases and the intervening interglacials.

The best preserved Eemian interglacial (MIS 5e) sediments in northern Fennoscandia occur in Leveäniemi, eastern Swedish Lapland (Lundqvist 1971; Robertsson 1991); Tepsankumpu, western Finnish Lapland (Saarnisto *et al.* 1999); Sokli, eastern Finnish Lapland (Helmens *et al.* 2000); Mertuanoja, west-central Finland (Nenonen 1995; Eriksson *et al.* 1999); and on the southern Kola Peninsula (Lunkka *et al.* 2018) (Fig. 1). At some of these sites, Saalian (MIS 6) till and glacifluvial sediments underlie the Eemian deposits (Hirvas 1991; Nenonen 1995; Lunkka *et al.* 2004; Svendsen *et al.* 2004; Johansson *et al.* 2011). There is only one site in northern Fennoscandia (Naakenavaara; Fig. 1) where the interglacial peat layer and the till unit beneath might have been deposited during the Holsteinian interglacial stage (MIS 11) and the pre-Holsteinian glacial phase, respectively (Hirvas 1991).

Stratigraphical evidence suggests that there were five SIS growth phases in western Finnish Lapland during the Weichselian. The SIS covered the area during the Herning (MIS 5d) and Rederstall (MIS 5a) interstadials, twice during the early Middle Weichselian (MIS 4 and MIS 3) and once during the Late Weichselian (MIS 2) substage (Johansson *et al.* 2011; Lunkka *et al.* 2014; Howett *et al.* 2015). However, the stratigraphical results indicate that the SIS covered eastern Finnish Lapland only four times during the Weichselian substages (Helmens *et al.* 2000, 2007; Lunkka *et al.* 2004, 2014; Johansson *et al.* 2011; Howett *et al.* 2015); once during the Rederstall stadial (MIS 5b), twice during the Middle Weichselian (MIS 4 and MIS 3), and once during the Late Weichselian (MIS 2); B, O and J reconstructions for MIS 5b in Fig. 2.

At several sites in southern and central Finland, south of the Oulu region (Fig. 1), Saalian, Eemian and

DOI 10.1111/bor.12560

Fig. 1. Location of the study area in eastern Fennoscandia and the Muhos site (black star) in the Oulu River Valley. Locations of the 22 stratigraphically important sites discussed in text are marked with numbered dots and listed below. The lines between Leveäniemi (site number 1) and the Last Glacial Maximum (LGM) position onshore Kuloi Plateau in the Arkhangel area (Transect A), and the line from Ajos (site number 22) to the LGM-limit in the Vologda region (Transect B) show the transects on which the glaciation curves in Fig. 2 are reconstructed. 1 = Leveäniemi; 2 = Tepsankumpu; 3 = Sokli; 4 = Mertuanoja; 5 = Varzuga; 6 = Naakenavaara; 7 = Rautuvaara; 8 = Hannukainen; 9 = Viitala; 10 = Vesiperä; 11 = Ukonkangas; 12 = Katosharju; 13 = Kostonniska; 14 = Permantokoski; 15 = Ossauskoski; 16 = Kauvonkangas; 17 = Vuojalankangas; 18 = Ruotanen; 19 = Vimpeli I; 20 = Horonkylä; 21 = Hangaskangas; 22 = Ajos.

Weichselian sediments have been discovered (Niemelä & Tynni 1979; Eriksson 1993; Nenonen 1995; Eriksson *et al.* 1999; Johansson *et al.* 2011; Lunkka *et al.* 2016). The most complete Eemian sediment beds occur at the Mertuanoja and Viitala sites (Fig. 1; Nenonen 1995; Eriksson *et al.* 1999), while only fragments of the Eemian strata are preserved elsewhere (Donner 1995). After the Eemian interglacial, the SIS covered the southern part of Finland during the early Middle Weichselian (MIS 4), late Middle Weichselian (MIS 3), and during the Late Weichselian (MIS 2) substages (Fig. 2; Nenonen 1995; Saarnisto & Salonen 1995; Lunkka *et al.* 2004, 2008, 2016; Saarnisto & Lunkka 2004; Johansson *et al.* 2011). However, Pitkäranta (2013) suggested that the SIS reached the westernmost part of southern Ostrobothnia during one of the Early Weichselian stadials (MIS 5b or MIS 5d).

Several studies have reconstructed the evolution of the SIS based on empirical data and modelling of the palaeo-ice sheet (Svendsen *et al.* 2004; Johnsen 2010; Olsen *et al.* 2013; Hughes *et al.* 2016; Batchelor *et al.* 2019). The different reconstruction techniques have often produced discrepant results, especially in terms of the extent and timing of the SIS coverage in its eastern flank (Sutinen 1992; Nenonen 1995; Saarnisto & Salonen 1995; Lunkka *et al.* 2004; Saarnisto & Lunkka, 2004; Svendsen *et al.* 2004; Sarala 2005; Johnsen 2010; Johansson *et al.* 2011; Olsen *et al.* 2013; Hughes *et al.* 2016; Batchelor *et al.* 2019; see also Fig. 2), which is mostly because of the lack of empirical data used in reconstructions. Upon comparing the present stratigraphical evidence of the Pleistocene history of northeastern Fennoscandia (i.e. Swedish and Finnish Lapland and the adjacent areas in northwest Russia) with the southern and central parts of Finland and northwest Russia (Figs 1, 2), it is evident that the correlation between these two areas is not straightforward. The application of the Eemian sediments as a marker horizon for correlating Late Pleistocene sediments from these areas is complicated because parts of the Eemian sedimentary successions are often eroded, reworked and /or glaciotectonized. However, the best preserved Eemian sites can be used for stratigraphical correlation to provide evidence if the SIS overran northern Finland during the Early Weichselian

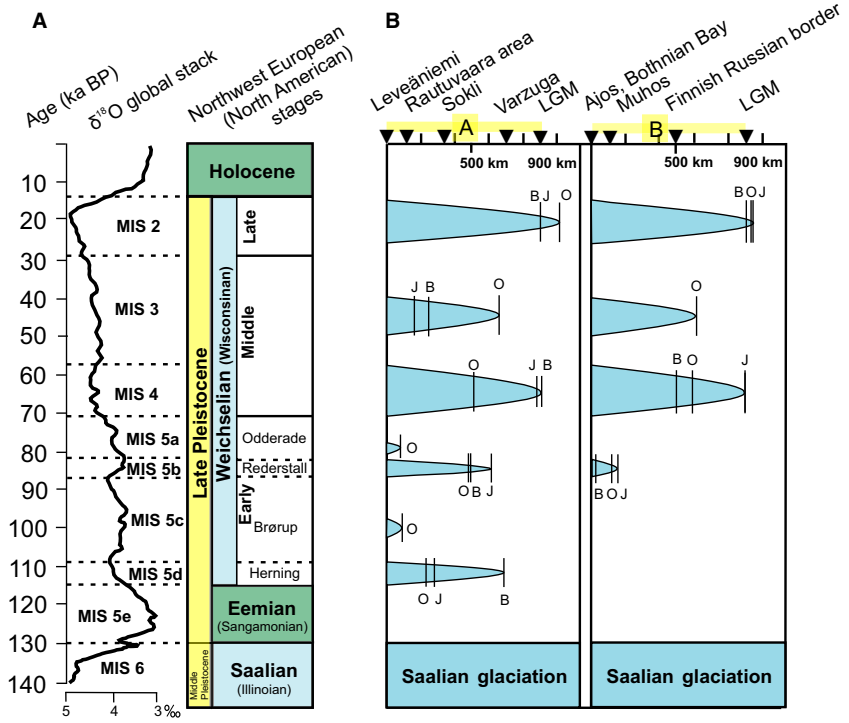

Fig. 2. A. Chronostratigraphical chart of the late Middle and the Late Pleistocene showing the comparison between the northwestern European terrestrial stages and substages and the marine isotope stages (MIS 6-2). The North American stages are in parentheses. The time scale on the left for the global benthic $\delta^{18}O$ stack and MIS is from Lisiecki & Raymo (2005). B. Glaciation curves showing SIS extent along two transects A and B (A: Leveäniemi – LGM on Kuloi Plateau and B: Ajos – LGM in the Vologda region, see Fig. 1) in the eastern flank of the SIS during the past ~140 ka. Three reconstructions of the SIS extent during the past ~140 ka are from J = Johnsen (2010); O = Olsen *et al.* (2013) and B = Batchelor *et al.* (2019). Vertical lines in the glaciation curves indicate the maximum ice limit of each reconstruction (J, O and B).

substages while southern Finland remained ice-free (Johansson *et al.* 2011).

The aims of this work are (i) to establish the Pleistocene stratigraphy and palaeoenvironmental history of the Oulu River valley area, where exceptionally thick Quaternary deposits rest on the Precambrian bedrock and (ii) to correlate the glacial events in the study area to the adjacent areas, and through that shed light on the SIS ice extent in the eastern part of Fennoscandia.

Study area

The Muhos core was drilled in the Oulu River valley (latitude 64.81°N, longitude 26.04°E, altitude ~29 m a.s.l.), situated at ~30 km from the shoreline of the Baltic Sea in western central Finland (Fig. 1). The bedrock of the Muhos drill-core site is composed of low-lying Neo- to Mesoproterozoic siltstone (the Muhos Formation; Tynni & Donner 1980; Tynni & Uutela 1984; Kesola 1985). The Muhos Formation is surrounded by higher ground where the bedrock is composed of Palaeoproterozoic granites, gneisses and schists (Fig. 3; Kesola 1985; Honkamo 1988). Late Pleistocene glacial deposits in the study area occur mostly as ground moraine. Streamlined glacial landforms such as drumlins and ribbed moraines oriented WNW to ESE are also commonly found in the area (Lunkka *et al.* 2013; Fig. 3). In addition, discontinuous, WNW to ESE-oriented esker chains also occur in the Oulu River valley. The western side of the Muhos area is characterized by low-relief modern topography that resulted from Holocene sedimentation of varved clays, silts, and organic-rich silts in the Oulu River basin during the Holocene Ancylus and Litorina stages of the Baltic Basin (Fig. 3). To the north and east of the Muhos site, the topography is relatively steep and rises by 70 m within 6 km (Fig. 3). As a result of the postglacial uplift, glacifluvial landforms were gradually elevated to the water level of the Baltic Basin, and affected by Holocene littoral processes forming for example, beach ridges (Fig. 3).

Material and methods

Drilling, OSL sampling, and sediment logging

The Geological Survey of Finland drilled a 54-m-deep sediment core at Muhos in 2006. The drilling site is located on the Muhos Formation ~1 km southwest from the contact to granite bedrock (Fig. 3). The core (Ø

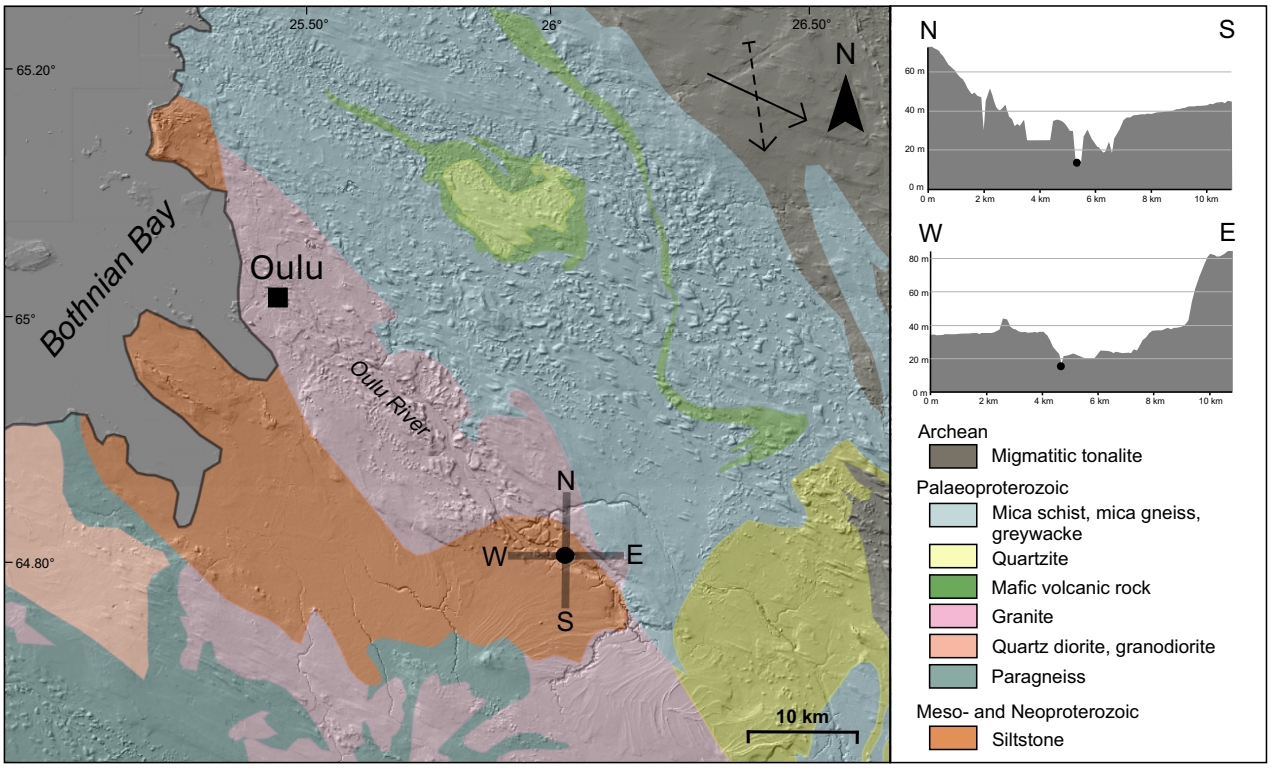

Fig. 3. DEM-imagery and bedrock map of the study area. The Muhos drilling site is located on the Muhos Formation siltstone. The Muhos Formation siltstone is surrounded by granitic-rocks, mica-rich schists and gneisses to the north, south and east, and granitoids to the west. Subglacial lineations and glacially abraded bedrock striations (Hakku service, digital data set of the Geological Survey of Finland, available at hakku.gtk.fi) are from two separate ice-flow directions; the older is from the NNW (dashed arrow) and the younger is from the WNW (solid arrow). The N–S and W–E land surface profiles crossing the drilling site (black dot on the map and in the profile) are shown in the top right corner of the figure. The low-relief topography rises relatively steeply to the north and east of the Muhos site (~70 m in 6 km). Bedrock map is modified from DigiKP, the digital bedrock database of the Geological Survey of Finland (available at gtkdata.gtk.fi/Kalliopera/index.html, DEM hillshade, National Land Survey of Finland).

50 mm) was drilled using a GM 200 GT pneumatic drilling platform with 1-m-long opaque sample tubes (plastic HDPV liners, Ø 40 mm) inside stainless-steel cover tubes. Continuous sampling was initiated from the ground surface. At 53.6 m below the ground surface (b.g.s.), the Muhos Formation siltstone was reached, and drilling was terminated at 54.0 m b.g.s. After successful core extraction, the sediment type at the top and bottom of each tube was recorded on site, and subsequently, the sample tubes were sealed with opaque plastic caps. Sample tubes from sand units for OSL dating were wrapped in aluminium foil and placed in black plastic bags.

The entire sediment sequence from the ground surface to the bedrock was cored with a 77% recovery. This percentage includes sediments obtained intact in cores (61% of the 54 m depth), unrecovered diamicton intervals, and sediments that were too fluid to remain intact. Fluid sediments were collected in sample bags. During drilling, it was observed that thick diamicton units occur below 30 m. Diamicton was easy to recognize because of its significantly higher drilling resistance compared to the sorted sediments. As a result, samples from only certain parts of the thick diamicton units were extracted.

The core tubes were split longitudinally in the Oulu University laboratory. The OSL sample tubes were opened under a low-level orange light and grain size of sediments estimated. Four OSL samples were taken from the bedded sand units at 24.30, 24.70, 39.70 and 39.30 m levels. After OSL sampling, a detailed sediment logging was made and samples for grain-size analysis were collected (Fig. 4). The sediment core is stored in the sediment laboratory at the Oulu Mining School, University of Oulu.

Fig. 4. Sediment log of the Muhos drill-core showing the six main sedimentary units discussed in text. The levels of the OSL and ^{14}C-dating samples are indicated with horizontal lines and ages are presented as kiloyears (ka). The diatom and pollen sample-levels are indicated with black squares. Dashed lines indicate sediment intervals not preserved in the core.

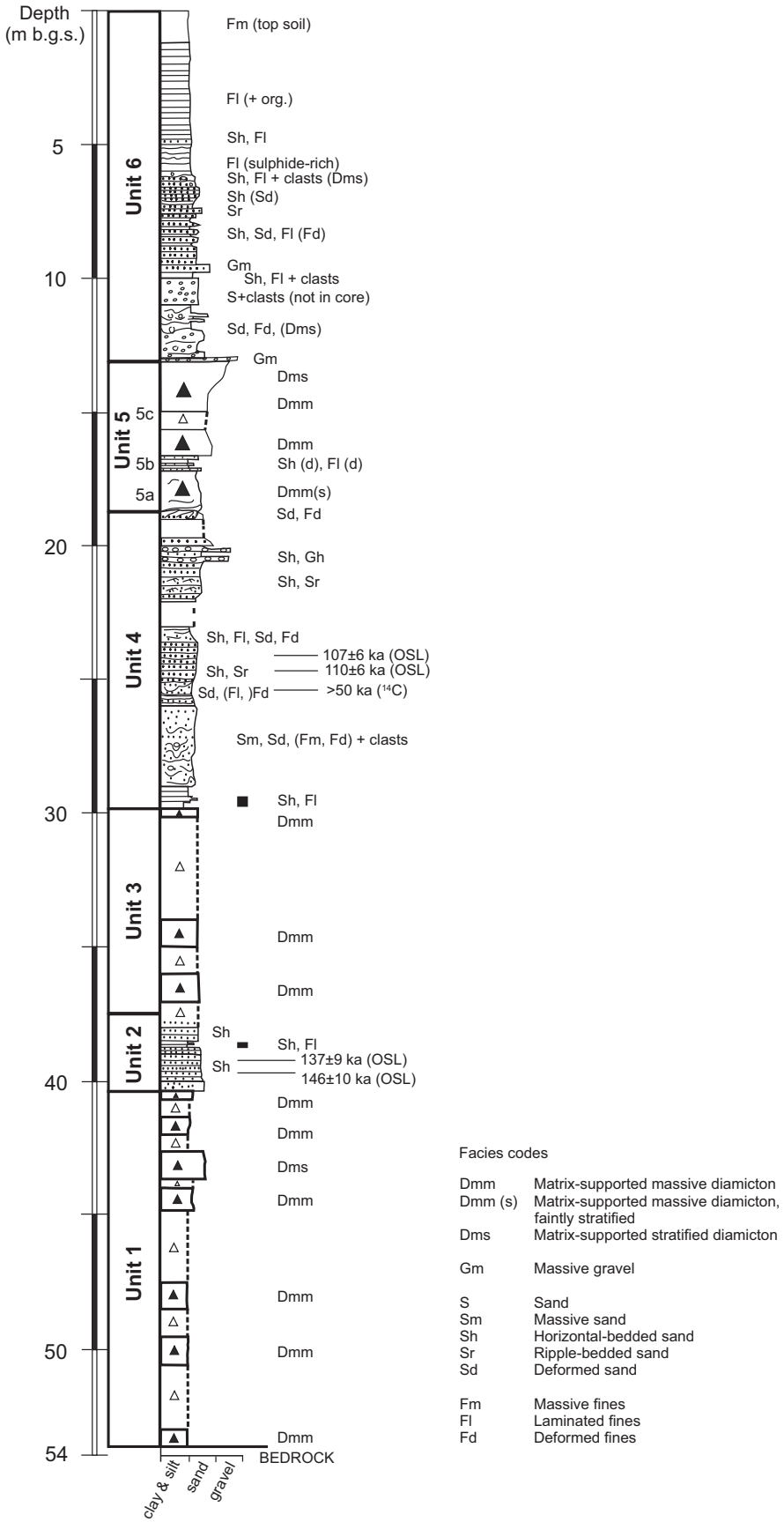

OSL and ^{14}C dating

The determination of OSL and ^{14}C AMS ages of the samples was carried out at the Nordic Laboratory for Luminescence Dating, Risø, Denmark (OSL samples) and the Poznan Radiocarbon AMS Laboratory in Poznan, Poland (^{14}C AMS samples).

In the OSL laboratory, the ends of the samples were retained for water content and dose rate analysis. The remaining portion was wet sieved to recover grains of 180–250 mm in diameter. This fraction was etched with HCl, H_2O_2, HF, and again with HCl to obtain a quartz-rich separate (Wintle 1997). After chemical separation, the samples exhibited a detectable IR-stimulated signal, indicating residual feldspar contamination. As a result, during routine measurement, all blue light stimulation was preceded by infrared stimulation at 125 °C (Wallinga *et al*. 2002).

OSL measurements were carried out using Risø OSL/TL readers, each equipped with a calibrated $^{90}Sr/^{90}Y$ beta radiation source and a blue (470±20 nm) light source (Bøtter-Jensen *et al*. 2000). The prepared quartz grains were attached in a monolayer to 10-mm-diameter stainless steel discs (with approximately a few thousand grains) using silicone oil. A SAR-protocol (Murray & Wintle 2000, 2003) was used to estimate all equivalent doses at 260 °C for 10 s and a cut heat of 160 °C. Dose rates were derived from radionuclide concentrations and were measured using high-resolution gamma spectrometry (Murray *et al*. 1987) considering conversion factors from Olley *et al*. (1996). These were modified by attenuation factors based on the observed sediment water content of 22–33% (Table 1). Finally, the internal alpha radiation contribution (assumed to be 0.06±0.03 Gy; Prescott & Hutton 1994) was added to the dose rates. The results of the OSL measurements are listed in Table 1. One ^{14}C-AMS age determination was performed on a wooden twig found in the sand unit at 25.6 m (Fig. 4, Table 1).

Diatom and pollen analysis

Diatom assemblages were determined from five diatom samples, collected from sediment intervals of 38.74–38.82 and 29.50–29.80 m. Diatoms were concentrated using the standard method described by Battarbee (1986). Organic matter was removed by oxidation with 40% H_2O_2, and coarse minerogenic matter was removed by decanting. The decanting procedure was repeated several times. Diatoms were mounted in Naphrax® and counted under a light microscope with an oil immersion objective having a magnification of 1000×. More than 400 diatom valves were counted. Diatom identification and taxonomy was mostly based on Krammer & Lange-Bertalot (1991a, b, 1997a, b), Mölder & Tynni (1967, 1968, 1973), Tynni (1975, 1978, 1980), Snoeijs (1993), Snoeijs & Vilbaste (1994), Snoeijs & Potapova (1995), Snoeijs & Kasperovičienė (1996) and Snoeijs & Balashova (1998). Taxonomic nomenclature was updated using AlgaeBase (Guiry & Guiry 2019).

Eight samples collected from 38.74–38.82 m and 31 samples collected from 29.50–29.80 m depths were subjected to pollen analysis. Approximately 1–2 g of sediment was used per pollen sample, and sampling was performed continuously at 1-cm intervals. The samples were treated with heavy liquids using LST Fastfloat, low-toxicity heteropolytungstates, at 1.95 g cm^{-3} (Eskola *et al*. 2021), boiled in 10% KOH, and were subsequently subjected to standard acetolysis. The concentrate was then mounted on silicone oil. *Lycopodium* tablets were added to the samples to calculate pollen concentrations. More than 500 terrestrial vascular pollen grains and spores were counted from each sample level whenever possible, at 400× magnification. At least half of each slide was counted to account for the uneven distribution of pollen and spores in the sample (Hicks 2001). Pollen identification was mainly based on Beug (2004), Reille (1998, 1999) and Moore *et al*. (1991). The terrestrial pollen sum (ΣP) was calculated based on trees, shrubs, dwarf shrubs and herbs. The percentage of aquatic plants, spores, and the green alga *Pediastrum* were calculated from the terrestrial pollen sum (ΣP) plus the sum of each group separately, for example, ΣP+aquatic plants. Unknown pollen were excluded from the pollen sum, and were counted separately (ΣP+unknown). The pollen diagram was drawn using Tilia software version 2.0.41 (Grimm 2018). Although pollen in most samples were well preserved, samples with broken and crumbled

Table 1. List of the OSL and ^{14}C-AMS dating results from the Muhos sediment core where laboratory codes (OSL Risø and ^{14}C-AMS Poznan), dated sample codes and their material as well as sample depth levels and sediment units are indicated. In the OSL data, dose and dose rate (equivalent dose, D_e) are listed. n = the number of individual aliquots contributing to D_e; w.c. = the saturated water content of the sediment samples.

Risø no./ Poznan no.	Sample code, material	Depth (m b.g.s.)/Unit	Dose (Gy)	Dose rate (Gy ka^{-1}; D_e)	n	w.c. (%)	OSL age (ka)/^{14}C age (a BP)
073201	M1, medium sand	24.00–24.30/Unit 4	204±7	1.90±0.08	23	23	107±6
073202	M2, medium sand	24.50–24.80/Unit 4	224±8	2.03±0.09	19	22	110±6
073211	M3, coarse sand	39.15–39.35/Unit 2	270±12	1.97±0.08	26	33	137±9
073212	M4, medium – coarse sand	39.75–39.50/Unit 2	308±15	2.11±0.09	30	27	146±10
Poz-20063	Muhos 1 – wooden twig	23.60/Unit 4					>50 000

pollen and also thin-walled pollen were counted separately. However, they were included in ΣP.

An attempt was made to distinguish the *Betula* tree and *Betula nana* based on their size and morphological characteristics (Birks 1968; Mäkelä 1996). It is known that the age and laboratory treatment methods affect the pollen grain size (Reitsma 1969; Fægri *et al*. 1989). All samples included a portion of distinctly smaller-sized pollen than that reported in the literature, which in some cases hindered reliable identification.

Results

Lithostratigraphy and dating results

The sediment succession above the bedrock is 53.6 m thick and can be divided into six lithostratigraphical units (Fig. 4).

Unit 1 (53.6–40.4 m b.g.s.) is a 13-m-thick massive diamicton (Fig. 4). Its colour varies between grey, red, and dark brown (Fig. 5A). Clasts are abundant in the red diamicton-type. The matrix of the upper, grey diamicton is coarser than that of the brown and red diamicton-types. Several superimposed diamicton beds are interpreted as lodgement and/or deformation till. However, it is impossible to evaluate whether each mineralogically and texturally distinct till bed corresponds to deposition during one or several glaciations.

Unit 2 (40.4–37.4 m b.g.s.) is mainly composed of parallel-bedded, coarse, medium and fine sands, including pebble gravel horizons, layers of laminated silt, and organic-rich silt (Fig. 4). The lower contact of Unit 2 is sharp. The lower part consists of coarse to medium sand, which fines upwards into laminated and massive organic-rich silt with a subordinate amount of clay (Fig. 5B). Parallel-bedded sand layers are 0.5–1.0 cm and the average silt laminae 0.2 cm thick. There was a massive (at places faintly laminated and deformed) fine to medium, poorly sorted sand layer above the organic-rich layer (Fig. 5B). The OSL ages of the medium and coarse sand (including fine gravel horizon) are 137±9 and 146±10 ka, respectively (Fig. 4, Table 1). Unit 2 was deposited in a lake basin. Parallel-bedded, coarse and medium sand could represent littoral, beach, or distal deltaic sands deposited in the basin, whereas fine sediments were deposited in deeper water. There is a massive and faintly stratified, fine to medium sand layer with subordinate amounts of silt overlying the laminated and organic-bearing silt layer, which could represent a massflow deposit owing to its massive structure, or a subglacially deformed sand and silt because it occurs below the diamicton unit. The latter interpretation is considered more likely.

Unit 3 (37.4–29.8 m b.g.s.) is more than 7 m thick and consists of massive sand diamicton (Figs 4 and 5C). Its basal contact was not preserved in the drill-core; however, the contact was defined by the changes in drilling resistance at 37.4 m. Matrix supported and massive diamicton with striated clasts is interpreted as lodgement or deformation till. It is most likely that the massive sand layer (in the upper part of Unit 2) beneath the till layer (Unit 3) is glaciotectonically homogenized and faintly deformed.

Unit 4 (29.8–18.6 m b.g.s.) is ~10 m thick (Fig. 4). It conformably overlies the diamicton (Unit 3). The basal part of the unit (29.83–29.55 m) is characterized by laminated clay, silt, and parallel-bedded fine sand layers with organic contents of less than 2% (Fig. 5D). A few small grains (3–5 mm in diameter) were also observed in the laminated basal unit. This laminated subunit grades upward into a 3.5-m-thick (29.5–26.0 m) massive and/or deformed (clay) silt and sand layer with occasional pebbles (Fig. 5E). Wood fragments are present in the deformed fine sand and silt between 25.5–25.6 m. Ripple and parallel-bedded sands and laminated silt occur between 25.0 and 19.0 m (Fig. 5F) above the deformed sand/silt unit. Unit 4 terminates with coarse sand, including two gravel layers occurring at 20.1 and 20.4 m that fine upwards into parallel-bedded sand between 20.1 and 18.6 m. A wood fragment at 25.5 m yields an infinite ^{14}C-AMS age (>50 ka) and two OSL ages determined at 24.2 m and 24.5 m yield ages of 107±6 and 110±6 ka, respectively (Fig. 4, Table 1). The laminated clay silt layer with parallel-bedded fine sand and occasional small clasts at the base of Unit 4 were deposited in a freshwater basin, probably in a glacial lake. The laminated structures, grain size, and low organic content suggest that the sediments were probably deposited in a relatively deep basin. The upward-fining massive and deformed sand and silt sets, including sporadic clasts overlying the laminated sediments, probably represent syndepositionally deformed lacustrine/glaciolacustrine sediments. Two cycles of parallel-bedded and ripple-bedded sands fining upward into deformed sands and silts indicate two sediment pulses into the lake basin. Overall, the upward-coarsening trend in the sediment succession indicates a lake basin infill and water level regression.

Unit 5 (18.6–13.2 m b.g.s.) is composed of diamicton, interbedded with 0.6-m-thick parallel-bedded sand and laminated silt (Fig. 4). The lower contact of the unit is gradational, and the underlying sand and silt in the top 0.3 m of Unit 4 deformed. The base (18.6–17.2 m) consists of weakly stratified sandy diamicton (subunit 5a in Figs 4, 5G), which grades into parallel- and ripple-bedded sand and laminated fines (17.2–16.6 m). This unit is overlain by massive sandy diamicton (16.6–13.3 m). The diamicton beds (subunits 5a and 5c in Fig. 4) are interpreted as lodgement tills. The contact between the sand beneath (top of Unit 4) and the lower diamicton in Unit 5 exhibits deformation similar to the contact between the upper till (subunit 5c) and the underlying sand (subunit 5b). Such deformed structures might have a

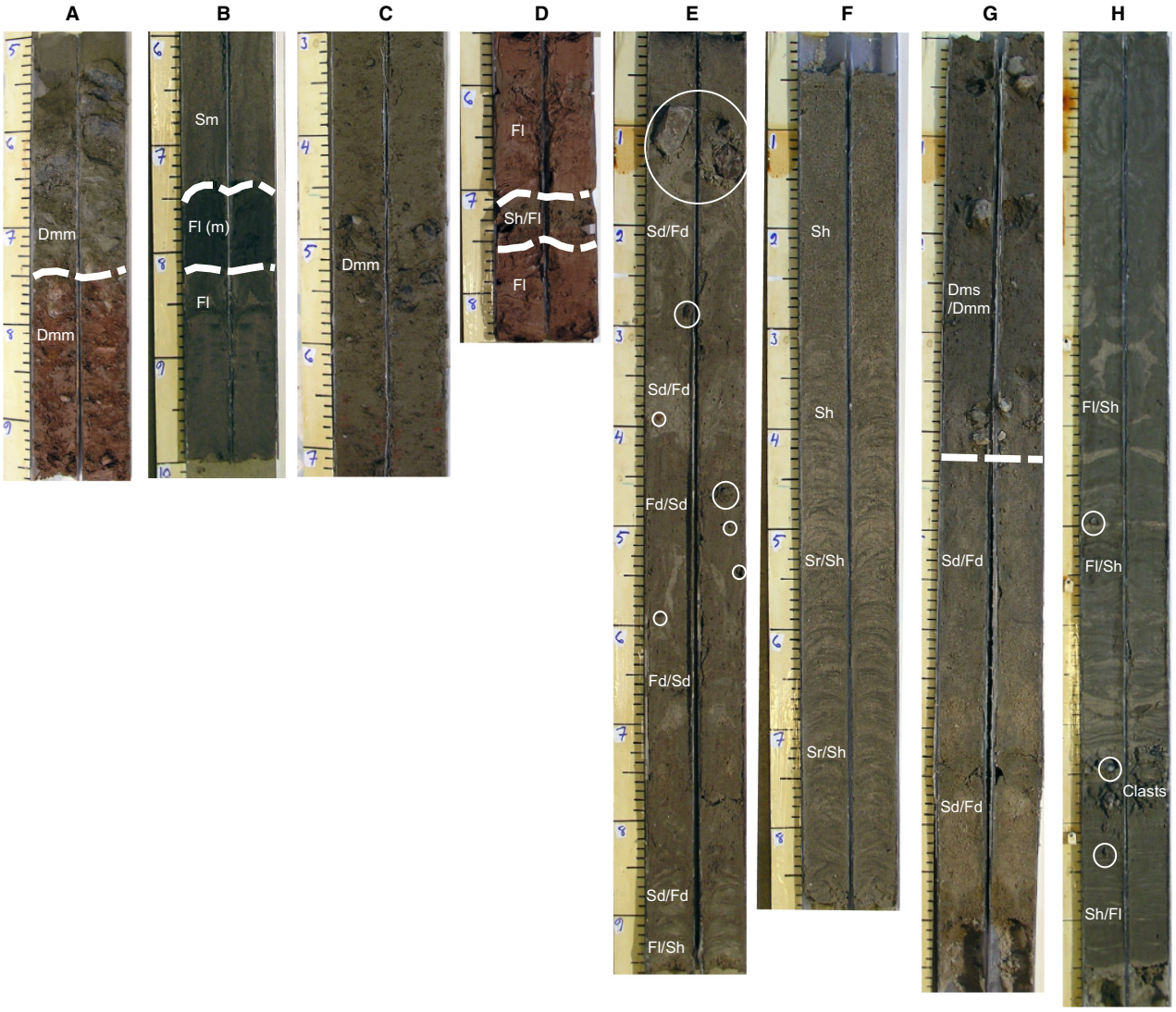

Fig. 5. Photographs showing examples of the Muhos drill-core sediments. A. Sediments between 41.50 and 41.97 m. A distinct colour change from red diamicton (lower) into the grey diamicton (upper) in Unit 1 at 41.75 m. B. Sediments between 38.0 and 37.60 m in Unit 2 where laminated silt and massive organic-rich silt are overlain by fine sand. Pollen and diatom analyses were performed on this blackish sediment interval. C. Massive sand diamicton (Unit 3) between 36.3 and 36.7 m. D. Sediments in the basal part of Unit 4 between 29.55 and 29.85 m showing reddish laminated silt and clay and a laminated fine sand and coarse silt bed in the middle. Pollen and diatom analyses were performed from this sediment interval. E. Deformed sand and silt in Unit 4 between 28 and 29 m with two embedded clasts. F. Rippled and parallel-bedded sand in the upper part of Unit 4 between 20 and 21 m. G. Gradational contact (white dashed line) between Unit 4 and Unit 5 at around 18.4–18.50 m. H. Glaciolacustrine (Ancylus Lake) laminated and syndepositionally deformed silt and fine sand with dropstone clusters and isolated dropstones in the lower part of Unit 6 between 9.0 and 10 m. Facies codes as in Fig. 4. Depth scale in cm. Photograph by J. Annanolli.

glaciotectonic origin caused by ice overriding the area twice, although it is difficult to deduce this from core exposure only. The genesis of partially tectonized, originally parallel- and ripple-bedded sands and fine silt lamina interbedded between two till units is difficult to interpret. Since sand layers (<1 cm thick) and silt laminae (a few millimetres thick) seem to alternate quite regularly, it is plausible that the sand-silt unit between the tills was deposited in a lacustrine rather than in a fluvial or aeolian environment, although the layer might have undergone deformation at a later stage.

Unit 6 (13.3–1.0 m b.g.s.) consists of an upward-fining sequence from gravel to laminated organic and clay-rich silt (Fig. 4). The lower contact was sharp. The base contains stratified gravel (13.3–12.9 m) overlain by a stratified mixture of deformed and laminated sand and silt with occasional clasts and clusters of clasts within a sand-silt matrix (12.9–11.0 m). Sand and silt with a few pebbles occur between 11.0–9.9 m overlain by deformed, laminated, parallel- and ripple-bedded sand and silt with isolated and clustered clasts (9.5–5.7 m) and dropstones (Fig. 5H). The top part of the unit is composed of laminated silt with occasional sulphide-

rich layers, and the organic content increased towards the top of the core. The upward-fining sediment sequence (Unit 6) from gravel and sand at the base to organic-bearing silt/clay represent a typical succession indicating deglaciation in an ice-contact glaciolacustrine basin, which subsequently became ice-free and part of the Baltic Basin waterbody (Ignatius *et al*. 1981). These sediments are thought to have been deposited in the Ancylus Lake and Litorina Sea of the Baltic Basin during the Holocene. The top 1 m of the core is composed of modern soil.

Diatom and pollen analyses and their environmental interpretation

Diatom assemblage. – Diatoms in Unit 2 (38.77 and 38.79 m) were heavily fragmented; however, the species or genus level could be still identified. Only the small taxa were found to be intact, and most of the other taxa were fractured. The diatom assemblage was composed mostly of planktonic freshwater taxa, dominated by *Aulacoseira islandica* and its resting spores (48–53%). Other *Aulacoseira* species, such as *A. granulata*, *A. subarctica*, *A. ambigua* and *A. lirata*, were also present. Several species of small Fragilariaceae, such as *Staurosira construens*, *S. venter*, *Staurosirella pinnata*, *S. lapponica*, *Pseudostaurosira brevistriata*, *Stephanodiscus rotula*, *Cyclotella schumannii* and *Achnanthes oestrupii*, were preserved. Sporadic frustules of *Fragilaria leptostauron* var. *martyi*, *Eunotia faba*, *Cocconeis* spp., *Cyclotella iris*, *Cymbella sinuata*, *Cymbella* spp., *Stephanodiscus minutulus* and *Tetracyclus glans* were identified. Several frustules and fragments of planktonic freshwater species *Cyclotella omarensis* and *Ellerbeckia arenaria*, *Epithemia* spp., *Diploneis* spp., *Didymosphenia geminata*, *Pinnularia* spp., *Stauroneis* spp., *Stephanodiscus* spp. and *Gomphonema* spp. fragments were also identified (Table 2).

The identified diatom assemblage entirely belongs to freshwater taxa, with the exception of a single frustule of the brackish water species, *Mastogloia smithii*. The diatom taxa are mostly planktonic, suggesting a deep-water environmental setting, and are comparable to the Holocene Ancylus Lake-phase diatom taxa of the Baltic Basin (Grönlund 1991a). The considerable presence of the cold-water species *A. islandica* and its resting spores indicate unfavourable conditions, such as limited light and temperature (Round *et al*. 1990; McQuoid & Hobson 1996). The small planktonic taxon *C. schumannii* has been reported from low-conductive lakes in northern Finland and Sweden, large lakes, mountain lakes, rivers (Cleve-Euler 1951; Håkansson 2002) and cold and deep lakes of Finnish Lapland (Sorvari *et al*. 2002). Small benthic Fragilariaceae (*Staurosira construens*, *S. venter*, *Staurosirella pinnata*, *S. lapponica*, and *Pseudostaurosira brevistriata*) are common species in alpine, sub-arctic and arctic lakes (Pienitz *et al*. 1995; Weckström *et al*. 1997; Laing *et al*. 1999; Lotter & Biegler 2000; Rühland *et al*. 2003). They could be also associated with colder and less productive conditions or lowering of the water level (Rühland *et al*. 2003), although small benthic Fragilariaceae are known to be environmentally tolerant taxa.

No diatom fragments or valves were found in the reddish clayey silt and silt sediment samples in Unit 4 at depths of 29.58, 29.66 and 29.79 m. The absence of diatoms might be associated with unfavourable conditions for diatom growth.

Since the laminated sediments at the base of Unit 4 were devoid of diatoms, we could not interpret the water quality into which laminated silt/clay/fine sand sediments were deposited. However, the laminated sediments normally accumulate in large basins with water depths exceeding 40 m (Ojala *et al*. 2013). Since the laminated sediments at the base of Unit 4 rest conformably on diamicton, it is likely that they were laid down in a glaciolacustrine setting.

Pollen assemblage. – The pollen assemblage at sample depths of 38.74–38.81 m in Unit 2 consisted of ~76 to 90% trees, 2–4% shrubs, 1–2% dwarf shrubs and 7–20% herb taxa (Fig. 6A). No significant changes occurred between the taxa within a sediment interval of only 8 cm. The pollen content was dominated by *Betula* trees (42–58%, including both thin-walled and worn *Betula* tree pollen grains) and *Pinus* (17–23%). *Alnus* (6–9%) and *Picea* (3–5%) were also constantly present. Thermophilous trees such as *Carpinus*, *Quercus*, *Tilia* and *Ulmus* occurred sporadically. Shrubs, such as *Betula nana*, *Corylus* and *Salix* and dwarf shrub taxa such as *Ledum* and *Vaccinium* were constantly present in low percentages. Cyperaceae (3–9%), Poaceae (2–7%) and *Artemisia* (maximum 2.3%) comprised the majority of the herb taxa. Spores of *Sphagnum* (11–16%), Polypodiaceae (3–6%), *Lycopodium* and *Equisetum* (~1%) were also constantly present. Single grains of *Osmunda* were found in the two samples. Aquatic species such as *Potamogeton*, *Sparganium*, *Myriphyllum*, *Isoetes*, *Nymphaea* and *Typha latifolia* occurred sporadically. The freshwater alga, *Pediastrum*, was also present throughout the sediment interval. The percentage of worn and degraded grains ranged from 5–18%. The maximum percentage of thin-walled grains was almost 13%, and it mostly consisted of triporate grains (*Betula* type). The total concentration of pollen and spores varied between ~80 000 and 330 000 grains g^{-1}.

An in-depth interpretation of the vegetation history of the region is difficult based on only an 8-cm sediment interval at the base of Unit 2. However, the pollen assemblage suggests that mixed forest with deciduous (birch and some alder) and coniferous trees (spruce and pine) existed around the freshwater basin. The sporadic occurrence of thermophilous tree pollen further complicated the interpretation, although it is most likely that

Table 2. Diatom taxa identified from the Muhos sediment samples, sample depths and percentages. Taxonomic nomenclature follows AlgaeBase (Guiry & Guiry 2019). Sampling depths of 29.58, 29.66 and 29.79 m were devoid of diatoms.

Diatom taxa	38.77 m	38.79 m
Achnanthes oestrupii (Cleve-Euler) Hustedt 1930	1.3	1.8
Achnanthes sp. Bory 1822	0.5	–
Amphora libyca Ehrenberg 1840	0.2	0.2
Amphora pediculus (Kützing) Grunow 1880	–	0.2
Aulacoseira ambigua (Grunow) Simonsen 1979	2.5	3.5
Aulacoseira granulata (Ehrenberg) Simonsen 1979	2.3	3.5
Aulacoseira islandica (O.Müller) Simonsen 1979	29.8	27.1
Aulacoseira islandica resting spores	18.2	25.9
Aulacoseira italica (Ehrenberg) Simonsen 1979	0.5	0.4
Aulacoseira lirata (Ehrenberg) Ross 1986	1.5	1.6
Aulacoseira sp. Thwaites 1848	1.8	0.4
Aulacoseira subarctica (O.Müller) Haworth 1990	3.5	1.2
Brachysira brebissonii R. Ross 1986	–	0.2
Cavinula cocconeiformis (Gregory ex Greville) D.G. Mann & A.J. Stickle 1990	–	0.6
Cavinula pseudoscutiformis (Hustedt) D.G. Mann & A.J. Stickle 1990	–	0.2
Cocconeis disculus (Schumann) Cleve 1882	0.2	–
Cocconeis lineata Ehrenberg 1849	0.3	–
Cocconeis neodiminuta Krammer 1991	0.2	–
Cocconeis sp. Ehrenberg 1838	0.2	–
Craticula subminuscula (Manguin) C.E. Wetzel & Ector 2015	0.2	–
Cyclotella iris Brun & Héribaud-Joseph 1893	2.6	0.4
Cyclotella michiganiana Skvortzow [Skvortzov] 1937	0.7	0.6
Cyclotella omarensis (Kuptsova) Loseva & Makarova 1977	1.5	1.2
Cyclotella radiosa (Grunow) Lemmermann 1900	0.2	0.2
Cyclotella schumannii (Grunow) Håkansson 1990	3.1	3.1
Cyclotella sp. (Kützing) Brébisson 1838	1.7	0.8
Cyclotella tripartita Håkansson 1990	–	0.2
Cymbella sp. Agardh 1830	0.3	–
Didymosphenia geminata (Lyngbye) M. Schmidt 1899	–	0.4
Discostella stelligera (Cleve & Grunow) Houk & Klee 2004	0.2	–
Ellerbeckia arenaria (Moore ex Ralfs) Crawford 1988	0.2	0.2
Epithemia turgida (Ehrenberg) Kützing 1844	0.3	–
Eunotia faba Ehrenberg 1838	0.8	0.2
Eunotia praerupta Ehrenberg 1843	0.2	0.2
Eunotia sp. Ehrenberg 1837	0.8	–
Fragilaria sp. Lyngbye 1819	1.3	0.6
Fragilariforma virescens var. *subsalina* (Grunow) Bukhtiyarova 1995	0.2	–
Gomphonema acuminatum Ehrenberg 1832	0.2	–
Gomphonema sp. Ehrenberg 1832	0.7	0.2
Hannaea arcus (Ehrenberg) R.M. Patrick 1966	0.2	0.2
Khursevichia jentzschii (Grunow) Kulikovskiy, Metzeltin & Lange-Bertalot 2012	0.2	0.4
Martyana martyi (Héribaud-Joseph) Round 1990	0.8	0.2
Navicula sp. Bory 1822	0.3	0.2
Pseudostaurosira brevistriata (Grunow) D.M. Williams & Round 1988	2.2	2.1
Reimeria sinuata (W. Gregory) Kociolek & Stoermer 1987	0.2	1.4
Staurosira binodis (Ehrenberg) Lange-Bertalot 2011	0.3	0.6
Staurosira construens Ehrenberg 1843	1.7	2.3
Staurosira venter (Ehrenberg) Cleve & J.D. Möller 1879	3.6	5.7
Staurosirella lapponica (Grunow) D.M. Williams & Round 1987	1.8	1.8
Staurosirella pinnata (Ehrenberg) D.M. Williams & Round 1988	6.3	5.1
Stephanodiscus medius Håkansson 1986	–	0.6
Stephanodiscus minutulus (Kützing) Cleve & Möller 1878	0.5	0.2
Stephanodiscus rotula (Kützing) Hendey 1964	1.8	1.8
Stephanodiscus sp. Ehrenberg 1846	–	0.6
Tabellaria sp. Ehrenberg 1840	0.3	–
Tetracyclus glans (Ehrenberg) Mills 1935	0.7	0.8
Unidentified	1.2	0.4

their occurrence might indicate either long-distance transport or redeposition. The presence of heavy spores of *Osmunda* indicated temperate climate because it grows in temperate and tropical areas worldwide (Birks & Paus 1991). Wetland taxa such as Cyperaceae, Poaceae and cryptogams were well preserved and were

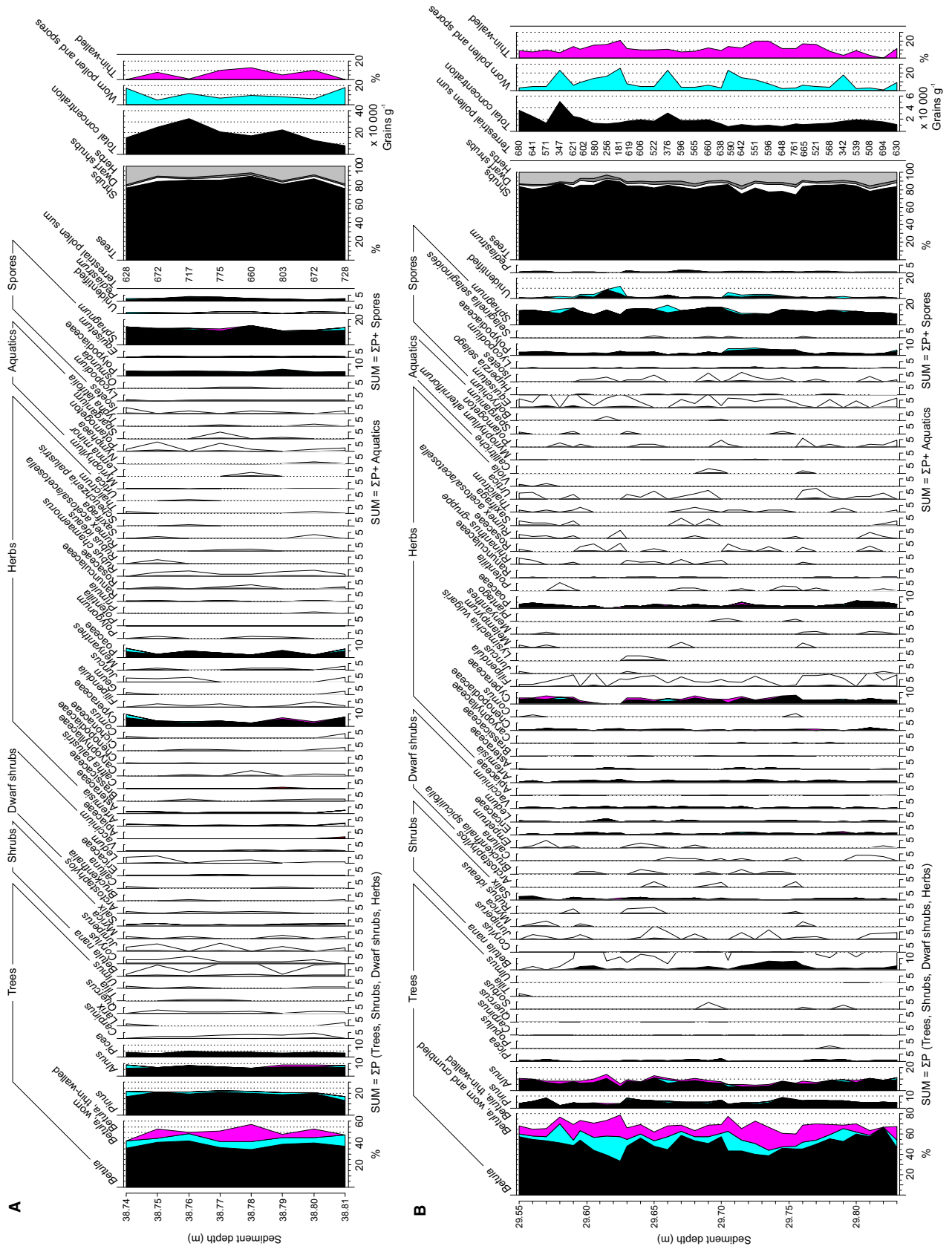

Fig. 6. Selected pollen and spore taxa with green alga *Pediastrum* from (A) Unit 2 and (B) Unit 4. Hollow curves represent 10× exaggeration. Turquoise curves indicate worn and crumbled pollen, purple curves indicate thin-walled pollen.

derived from the shore areas of the basin. Based on the plant indicator species, the presence of thermophilous aquatic plants *Nymphaea* and *Typha*, if deposited *in situ*, indicates minimum July temperatures >13 °C and >15 °C, respectively, in the study area (Väliranta *et al.* 2015 and references therein).

The pollen assemblage in Unit 4 at sample depths of 29.55–29.83 m consists of trees (74–91%), shrubs (1–9%), dwarf shrubs (1–4%) and herbs (3–15%) (Fig. 6B). The major tree taxa are *Betula* (60–79%), *Alnus* (5–14%) and *Pinus* (2–9%). *Picea* is constantly present with low percentages (0.2–1.7%), and other trees such as *Carpinus*, *Quercus*, *Sorbus*, *Tilia* and *Ulmus* occur as single grains. *Betula nana* is the most common shrub with a value ranging from 0 to 7.6% and *Salix* has an occurrence of up to 3%. *Vaccinium* and *Ledum* are the most common dwarf shrubs with low percentages, and *Empetrum*, *Calluna* and *Bruckenthalia spiculifolia* occur as single grains. Cyperaceae (0–8%), Poaceae (0–6%), *Artemisia* (0–2%), *Filipendula* and Chenopodiaceae are the most common herb taxa. The most common aquatic species are *Potamogeton* and *Myriophyllum*, with sporadic presence of *Sparganium*. The freshwater alga, *Pediastrum*, is low in abundance. *Sphagnum*, Polypodiaceae, *Equisetum*, *Lycopodium* and the aquatic plant *Isoetes* comprise the majority of the spore-forming taxa. The percentage of worn and degraded pollen and spore grains ranged from 1–26%, and the maximum percentage of thin-walled grains was 21%. The majority of these degraded and thin-walled pollen are *Betula*-type pollen grains, and it may also include *Betula nana* pollen. The total concentration of pollen and spores varies from 7000–51 000 grains g^{-1}, which is merely a tenth of the concentration at sampling depth of 38.74–38.81 m.

The pollen assemblage suggests taxa typical of interstadial phase vegetation around the basin where sediments were deposited. A relatively high abundance of *Betula* tree and *Alnus*, a relatively low percentage of non-arboreal pollen (NAP), and low abundance of *Betula nana*, *Salix*, *Artemisia* and Poaceae suggest a forested environment with birch, alder, and perhaps scattered pine. It is likely that the sporadic pollen-grain occurrences of thermophilous trees such as *Carpinus*, *Quercus*, *Tilia* and *Ulmus* reflect their long-distance origin or redeposition. The presence of *Salix*, Cyperaceae, *Filipendula*, Poaceae and cryptogams reflects the type of vegetation that existed on the shore of the basin.

Discussion

The sedimentary succession of the Muhos core exhibits four till units interbedded with sands and less abundant silt, clay, gravel, and two organic-rich intervals. Four till units (Units 1, 3, 5a and 5b; Fig. 4) indicate that the Muhos and adjacent areas were covered by the SIS four times prior to the Holocene, and the Bothnian Bay sediments (Unit 6) were deposited during this period. The lithological and mineralogical composition of the lowermost till complex (i.e. Unit 1) has been previously studied by Lunkka *et al.* (2013). The study shows that the dark brown till beds containing abundant mica schists, mica gneisses, and mafic volcanic clasts reflect a northern provenance of the clasts, i.e. ice movement was from the north. In contrast, the grey and red till beds containing abundant granite and siltstone clasts indicate a western provenance, i.e. the ice flow was from the west to the Muhos area. Two OSL samples from Unit 2 situated above the till complex (Unit 1) yielded ages of 137±9 and 146±10 ka, suggesting that the till complex beneath Unit 2 was deposited during the late Saalian (MIS 6) glaciation (Fig. 7). However, it is also plausible that the till complex (Unit 1) represents till beds deposited not only during the late Saalian glaciation but also during earlier glacial phases.

Unit 2, with littoral sands at the base overlain by deep-water organic fine-grained sediments and deformed sands above (Fig. 4), was deposited in a lake. The OSL results indicate that the maximum age for the deposition of littoral sands is 137±9 ka. The presence of freshwater diatom taxa in the laminated silt supports the environmental interpretation. In addition, the presence of a green alga, *Pediastrum*, throughout the laminated silt layer reflects sedimentation in a lacustrine basin. *Pediastrum*, along with the abundant planktonic taxon *A. islandica* and small benthic Fragilariaceae taxa, indicate that a cool, non-saline lake existed when the laminated sediments were deposited. Although the dominance of resting spores of *A. islandica* might not necessarily indicate a deep-water environment (Peltoniemi *et al.* 1989), the presence of laminated silt rhythmites and planktonic diatom taxa indicate deposition in a relatively deep lacustrine environment.

Western Finland, including the Muhos area, was inundated by the Eemian Sea during the Eemian interglacial (Forsström *et al.* 1988; Grönlund 1991b). The estimated water level of the Eemian Sea in central western Finland adjacent to the Gulf of Bothnia was ~110 m a.s.l. (Forsström *et al.* 1988; Fig. 1). Since there are no marine diatom taxa apart from a single frustule of a brackish water taxon (i.e. *Mastogloia* sp.), the silt and clay interval in Unit 2 cannot be correlated with the high water level Eemian Sea phase. Therefore, it is suggested that the laminated silt and clay were deposited during the early or late Eemian freshwater phase, which either preceded or post-dated the Eemian Sea phase. However, the pollen data contradict the correlation with the early Eemian freshwater phase. The pollen assemblage includes abundant conifers and grains of thermophilous trees with sporadic occurrence of *Osmunda*. However, the pollen taxa are not dominated by birch, as is the case for the pollen taxa in Haapavesi (Vesiperä site), Peräseinäjoki (Viitala site) (Nenonen *et al.* 1991) and Ylivieska (Mertuanoja site) (Eriksson *et al.* 1999; Fig. 1), which represent early Eemian freshwater lacus-

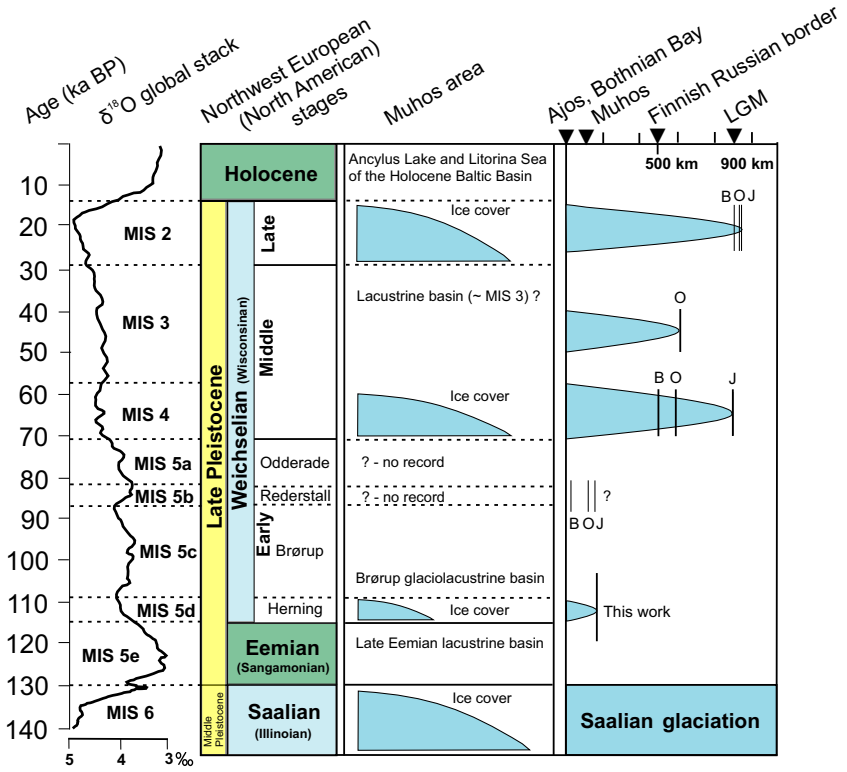

Fig. 7. Glaciation and environmental history of the Muhos area and the time-distance diagram of the SIS from the Saalian to the Holocene. The North American stages are expressed in parentheses. See Fig. 1 for the explanation of chronostratigraphy and the abbreviations in the distance diagram.

trine sediments with diatom taxa similar to those of Unit 2 at Muhos.

Pollen and diatom evidence from the Ukonkangas site, Kärsämäki (Fig. 1), only 100 km south of the Muhos site, suggests that the upper sediment units at the Ukonkangas site were deposited during the end of the temperate Eemian interglacial (Grönlund 1991b; Eriksson 1993). The pollen data from the silt-rich sediments show similar characteristics as those studied at Muhos, with the exception of slightly lower spruce and pine and greater abundance of alder. *Quercus* and *Corylus* are ubiquitously present at the Ukonkangas site, whereas their occurrence in Muhos is sporadic. The diatom taxa from the sediments of the Ukonkangas site show a transition from the brackish Eemian Sea to freshwater conditions (Grönlund 1991b). Therefore, the lake sediments in Unit 2 at Muhos can be correlated to the late Eemian lacustrine sediments of the Ukonkangas site.

The littoral sands at the base of Unit 2 with the OSL age of 137±9 ka (Fig. 4) may represent sands deposited during the transition from the Saalian glaciation to the Eemian interglacial. However, the OSL age uncertainty due to systematic and random errors, such as a spread in equivalent doses and uncertainty in water content fluctuations and burial history, can be significantly large (higher than 10%) (Wallinga & Cunningham 2015). Therefore, it is tentatively suggested that these sands represent littoral deposits that were laid down when the lake basin isolated from the Eemian Sea due to glacio-isostatic uplift. The silt and clay above represent deeper freshwater facies of the basin that was subsequently uplifted and filled with sands (Figs 4, 7).

Lodgement till (Unit 3) indicates that the SIS overrode the Muhos region. Although the application of till clast lithology to trace the direction of ice movement is ambiguous, a significantly high proportion (>50%) of mica gneiss, quartzite, and mafic volcanic clasts in this till unit (Lunkka *et al*. 2013) might reflect ice movement from the N or NW. Since the sands in Unit 4 have ages of 107±6 and 110±6 ka (Fig. 4, Table 1) and the lake sediments in Unit 2 were deposited during the late Eemian, it is most likely that the till (Unit 3) was deposited by the SIS during the Early Weichselian Herning stadial (MIS 5d). This indicates that the SIS had extended further to the south than previously thought (Sutinen 1992; Nenonen 1995; Saarnisto & Salonen 1995; Lunkka *et al*. 2004; Svendsen *et al*. 2004; Sarala 2005; Johansson *et al*. 2011; Olsen *et al*. 2013; Batchelor *et al*. 2019; Fig. 7).

The glaciolacustrine sediments in Unit 4 exhibit a succession that represents deep to shallow water facies (Fig. 4). Small dropstones in laminated fine sediments at

the base most likely represent rain-out from melting icebergs in the glaciolacustrine basin or grains that were transported by lake ice during melting seasons. The occurrence of deformed sediments above the laminated unit indicates that the sediment source became more proximal with intermittent input events of coarse sediments. For example, input from collapsed deltaic sediments or riverine input may have caused syndepositional deformation in finely laminated sediments deposited during quiet periods. Two OSL ages and one infinite ^{14}C age (Table 1) obtained from the gravel and sand layer above the basal rhythmites, and the deformed beds suggest that the laminated deep-water sediments were deposited during the early part of the Brørup interstadial (MIS 5c) (Fig. 7).

The pollen content of the fine sediment interval at the base of Unit 4 is dominated by birch with subordinate pine and alder (Fig. 6B). The pollen assemblage is monotonous throughout the sediment interval, and therefore it is difficult to correlate with other subtill sediment pollen assemblages in the region. Birch-dominated subtill, organic-bearing pollen sites with minor (or absent) pine, spruce and alder have been reported from Pudasjärvi (Katosharju site; Sutinen 1992; Sarala *et al.* 2006) and Taivalkoski (Kostonniska site; Korpela 1969) in the northern part of the North Ostrobothnian Province and at several sites in southern Lapland (Permantokoski, Ossauskoski and Kauvonkangas sites; Fig. 1; Korpela 1969; Mäkinen 2005). The interstadial-type sediments at these sites represent the Peräpohjola interstadial (Korpela 1969), which was previously correlated with the Early Weichselian interstadials Brørup (MIS 5c) or Odderade (MIS 5a). However, later studies have suggested its correlation with the Middle Weichselian interstadials (MIS 3; Johansson *et al.* 2011). The pollen assemblage of Unit 4 at Muhos differs from the pollen assemblage of the Peräpohjola interstadial sites in terms of higher relative proportions of alder and conifers and a lower proportion of NAP.

South of the Muhos site, the birch-dominated pollen assemblages from the organic-rich sediments of the Oulainen (Vuojalankangas site) (Forsström 1982, 1988; Nenonen 1995), Pyhäsalmi (Ruotanen site; Nenonen 1995), Vimpeli (Vimpeli I site; Aalto *et al.* 1983, 1989) and Teuva regions (Horonkylä site; Nenonen 1995; Grönlund & Ikonen 1996) (Fig. 1) were deposited during the Early Weichselian Brørup interstadial (Donner 1995; Nenonen 1995). The pollen assemblage of the laminated sediment interval in Unit 4 cannot be directly correlated with the pollen assemblages of the Brørup interstadial sites mentioned above. However, at Sokli (Fig. 1), a composite sediment core covering the last interglacial–glacial cycle is preserved (Helmens *et al.* 2000), and the initiation of the MIS 5c (Brørup) (Sub-zone II a; Helmens *et al.* 2012) gyttja shows a pollen assemblage similar to that at Muhos. This indicates that a sub-arctic birch forest with alder and possible conifers was present in the Sub-zone II a, i.e. during the beginning of the MIS 5c. The higher proportion of *Alnus* at Muhos may also indicate moist conditions around the local lake basin.

It is evident that the fine-sediment interval at the base of Unit 4 partially exhibits an interstadial succession. Furthermore, the counts of worn and thin-walled pollen are relatively large, and they might include *Betula nana*. Therefore, the redeposition of at least some pollen and spores cannot be disregarded. Based on the overall sedimentary succession, pollen, and the OSL age, we suggest that the fine sediment interval and the associated sands and gravels were deposited during the Brørup interstadial.

Unit 5 is a composite unit consisting of two till beds (subunits 5a and 5c in Fig. 4) interbedded with parallel- and ripple-bedded sand and laminated silt (subunit 5b in Fig. 3). This sedimentary succession indicates that there were possibly two ice advances across the area separated by one ice-free period (Fig. 7). Based on lithological analyses of tills in Unit 5, Lunkka *et al.* (2013) suggested that the clasts in the lower till bed (subunit 5a) are predominantly mica schists and mica gneiss, while granite clasts dominate the lithological composition of the upper till bed (subunit 5c). This difference, together with ice flow direction data (cross-cutting bedrock striations and cross-cutting landform lineation patterns; see Fig. 3) indicate that there was an older ice advance from the north, and subsequently a younger one from the NW direction. In the Hangaskangas, Katosharju and Ajos sites situated at 15 km NW, 50 km NE and 120 km NW of the Muhos site, respectively (Fig. 1), sands beneath the uppermost till are of Middle Weichselian age (OSL ages 41.6, 49.2 and 46 ka, respectively), and the till clast fabric results indicate that the uppermost till was deposited during a westerly ice-flow phase (Sutinen 1992; Bargel *et al.* 1999; Pasanen & Lunkka 2008). Therefore, we tentatively correlate the lower till (subunit 5a) with the first Middle Weichselian ice growth phase (MIS 4), the sand and silt (subunit 5b) between the two till beds with the Middle Weichselian interstadial (MIS 3), and the upper till (subunit 5c) with the Late Weichselian ice growth phase.

Unit 6, with its basal conglomerate grading upwards into mass movement and sub-aqueous glacifluvial and glaciolacustrine sediments, represents a typical sedimentary succession deposited during the Ancylus Lake phase of the Baltic basin as the ice retreated from the area (Ignatius *et al.* 1981). Organic- and sulphide-rich laminated and massive silt above the Ancylus sediments most likely represents the Litorina stage sediments of the Baltic Basin.

Overall, the sediment successions at Muhos and the adjacent sites demonstrate that after the Saalian glaciation, the Eemian Sea inundated the coastal areas of the Gulf of Bothnia. Due to the glacio-isostatic uplift following the Saalian glaciation, the Muhos area was

eventually uplifted to the contemporary Eemian Sea level. At that time, littoral processes must have eroded the existing Eemian Sea sediments, and sands and gravels remained as littoral deposits in the area (Nenonen 1995). Subsequently, a lake basin was isolated from the Eemian Sea and the lacustrine sediments in Unit 2 were deposited.

The first ice advance into the Muhos area in the Weichselian took place during the Herning stadial (MIS 5d). According to earlier studies (Lunkka *et al*. 2013), this ice advanced from the north. However, the extent of this ice south of the Muhos region is uncertain. Since a till unit deposited during the Herning stadial occurs at the Muhos site and in western Lapland (Rautuvaara and Hannukainen sites), but not in eastern Finnish Lapland (Sokli site), the ice margin must have covered large areas in western Lapland and central Finland (Fig. 7). There has been no evidence of a Herning stadial ice advance to the central and southern parts of Finland. Therefore, the till (Unit 3) between the late Eemian lacustrine sediments (Unit 2) and the dated sands (Unit 4) at Muhos is the first stratigraphically controlled and age-bracketed evidence of an ice advance into central Finland during the Early Weichselian Herning stadial. These results suggest that the extent of the ice sheet was underestimated in former studies, at least in the southeastern flank of the SIS during the Early Weichselian (MIS 5d) substage.

A lake, probably a part of a large glacial lake in the Bothnian Bay of the Baltic Basin existed in the Muhos area during the early part of the Brørup interstadial and the SIS covered the area three times after the Brørup interstadial. Although the biostratigraphical and geochronological evidence from the Muhos core sediments is limited, information from adjacent sites such as Kauvonkangas (Mäkinen 2005), Hannukainen (Howett *et al*. 2015) and Mertuanoja (Nenonen 1995) suggests that the SIS covered the area twice during the Middle Weichselian (MIS 4 and MIS 3) and once during the Late Weichselian (MIS 2) stage (Fig. 7).

Conclusions

- The 54-m-long Muhos sediment core studied in the Oulu River valley, central western Finland, situated adjacent to the centre of the SIS, displays multiple till units interbedded with organic-rich clays, silts, sands and gravels. The core covers a time-span from the Saalian (MIS 6) glaciation to the Holocene.
- The results of the Muhos core indicate that there were at least four ice advances across the Muhos area. Based on the OSL results and biostratigraphical evidence, the oldest ice advance took place during the late Saalian stage, and the subsequent advances during the Early Weichselian, Middle Weichselian and Late Weichselian.
- The sediment record indicates that a freshwater basin existed in the Muhos area during the late Eemian interglacial, Brørup interstadial, and possibly also during the Middle Weichselian interstadial as well as during the Holocene Ancylus Lake phase of the Baltic Basin.
- In contrast to the previous estimations of the SIS extent during the Early Weichselian, the results of this study show that the SIS overran the Muhos area from the north and advanced into central Finland during the Early Weichselian Herning stadial.

Acknowledgements. – The Geological Survey of Finland is acknowledged for providing the drill-core used in this study. Riitta Kontio is thanked for providing help with pollen preparation. We thank Stephen Nelson, an anonymous reviewer, and the editor Jan A. Piotrowski for their valuable comments that helped to improve the manuscript. The authors declare that there are no conflicts of interest with third parties.

Author contributions. – JPL designed the study with contributions from TE. TE and JPL wrote the manuscript. TE performed the pollen and diatom analyses, and JPL performed the sedimentological analysis. Both TE and JPL contributed to the interpretation of the data and the drafting of this manuscript.

References

Aalto, M., Donner, J., Hirvas, H. & Niemelä, J. 1989: An interglacial beaver dam deposit at Vimpeli, Ostrobothnia, Finland. *Geological Survey of Finland Bulletin 348*, 34 pp.

Aalto, M., Donner, J., Niemelä, J. & Tynni, R. 1983: An eroded interglacial deposit at Vimpeli, South Bothnia, Finland. *Geological Survey of Finland Bulletin 324*, 43 pp.

Bargel, T., Huhta, P., Johansson, P., Lagerøäck, R., Mäkinen, K., Nenonen, K., Olsen, L., Rokoengen, K., Svedlund, J.-O., Väänänen, T. & Wahlroos, J.-E. 1999: *Maps of Quaternary Geology in Central Fennoscandia, Sheet 3: Ice-flow indicators, scale 1:1 000 000 and Quaternary Stratigraphy, scale 1: 2 000 000*. Geological Surveys of Finland (Espoo), Norway (Trondheim) and Sweden (Uppsala).

Batchelor, C. L., Margold, M., Krapp, M., Murton, D. K., Dalton, A. S., Gibbard, P. L., Stokes, C. R., Murton, J. B. & Manica, A. 2019: The configuration of Northern Hemisphere ice sheets through the Quaternary. *Nature Communications 10*, 3713. https://doi.org/10.1038/s41467-019-11601-2.

Battarbee, R. W. 1986: Diatom analysis. *In* Berglund, B. E. (ed.): *Handbook of Holocene Palaeoecology and Palaeohydrology*, 527–570. Wiley & Sons Ltd, Chichester.

Beug, H.-J. 2004: *Leitfaden der Pollenbestimmung für Mitteleuropa und angrenzende Gebiete*. 542 pp, Verlag Friedrich Pfeil, Munich.

Birks, H. H. & Paus, A. 1991: Osmunda regalis in the early Holocene of Western Norway. *Nordic Journal of Botany 11*, 635–640.

Birks, H. J. B. 1968: The identification of Betula nana pollen. *New Phytologist 67*, 309–314.

Bøtter-Jensen, L., Bulur, E., Duller, G. A. T. & Murray, A. S. 2000: Advances in luminescence instrument systems. *Radiation Measurements 32*, 523–528.

Cleve-Euler, A. 1951: Die Diatomeen von Schweden und Finland. *Kungliga Svenska Vetenskapsakademiens Handlingar 2*, 163 pp.

Donner, J. 1995: *The Quaternary History of Scandinavia*. 200 pp, Cambridge University Press, Cambridge.

Eriksson, B. 1993: The Eemian pollen stratigraphy and vegetational history of Ostrobothnia, Finland. *Bulletin of the Geological Survey of Finland 372*, 36 pp.

Eriksson, B., Grönlund, T. & Uutela, A. 1999: Biostratigraphy of Eemian sediments at Mertuanoja, Pohjanmaa (Ostrobothnia), western Finland. *Boreas 28*, 274–291.
Eskola, T., Kontio, R. & Lunkka, J. P. 2021: Comparison between modified LST Fastfloat and conventional HF methods for pollen preparation in highly minerogenic sediments. *Bulletin of the Geological Society of Finland 93*, 5–18.
Fægri, K., Iversen, J., Kaland, P. E. & Krzywinski, K. 1989: *Textbook of Pollen Analysis*. 328 pp. Wiley, London.
Forsström, L. 1982: The Oulainen interglacial in Ostrobothnia, western Finland. *Acta Universitatis Ouluensis, Series A, Scientiae Rerum Naturalium 136, Geologica 4*, 116 pp.
Forsström, L. 1988: The northern limit of pine forest in Finland during the Weichselian interstadials. *Annales Academiae Scentiarum Fennicae, Series A III 147*, 24 pp.
Forsström, L., Aalto, M., Eronen, M. & Grönlund, T. 1988: Stratigraphic evidence for Eemian crustal movements and relative sea-level changes in eastern Fennoscandia. *Palaeogeography, Palaeoclimatology, Palaeoecology 68*, 317–335.
Grimm, E. C. 2018: *TILIA software version 2.0.41*. Illinois State Museum, Research and Collection Center, Springfield, USA.
Grönlund, T. 1991a: The diatom stratigraphy of the Eemian Baltic Sea on the basis of sediment discoveries in Ostrobothnia, Finland. *Geological Survey of Finland, Reports of Investigations 102*, 26 pp.
Grönlund, T. 1991b: New cores from Eemian interglacial deposits in Ostrobothnia, Finland. *Geological Survey of Finland Bulletin 352*, 31 pp.
Grönlund, T. & Ikonen, L. 1996: Early Weichselian biostratigraphy and vegetational development at Horonkylä, Pohjanmaa, Western Finland. *Bulletin of the Geological Society of Finland 68*, 68–84.
Guiry, M. D. & Guiry, G. M. 2019: *AlgaeBase*. National University of Ireland, Galway. http://algaebase.org.
Håkansson, H. 2002: A compilation and evaluation of species in the general *Stephanodiscus*, *Cyclostephanos* and *Cyclotella* with a new genus in the family Stephanodiscaceae. *Diatom Research 17*, 1–139.
Helmens, K. F., Johansson, P. W., Räsänen, M. E., Alexanderson, H. & Eskola, K. O. 2007: Ice-free intervals continuing into Marine Isotope Stage 3 at Sokli in the central area of the Fennoscandian glaciations. *Bulletin of the Geological Society of Finland 79*, 17–39.
Helmens, K. F., Räsänen, M., Johansson, P. W., Jungner, H. & Korjonen, K. 2000: The Last Interglacial – Glacial cycle in NE Fennoscandia: a nearly continuous record from Sokli (Finnish Lapland). *Quaternary Science Reviews 19*, 1605–1623.
Helmens, K. F., Väliranta, M., Engels, S. & Shala, S. 2012: Large shifts in vegetation and climate during the Early Weichselian (MIS 5d-c) inferred from multi-proxy evidence at Sokli (northern Finland). *Quaternary Science Reviews 41*, 22–38.
Hicks, S. 2001: The use of annual arboreal pollen deposition values for delimiting tree-lines in the landscape and exploring models of pollen dispersal. *Review of Palaeobotany and Palynology 117*, 1–29.
Hirvas, H. 1991: Pleistocene stratigraphy of Finnish Lapland. *Geological Survey of Finland Bulletin 354*, 123 pp.
Honkamo, M. 1988: *Bedrock map of Haukipudas and Kiiminki areas. Geological map of Finland 1:100 000, sheets 2533 and 3511*. Geological Survey of Finland, Espoo.
Howett, P. J., Salonen, V.-P., Hyttinen, O., Korkka-Niemi, K. & Moreau, J. 2015: A hydrostratigraphical approach to support environmentally safe siting of a mining waste facility at Rautuvaara, Finland. *Bulletin of the Geological Society of Finland 87*, 51–66.
Hughes, A. L. C., Gyllencreutz, R., Lohne, Ø. S., Mangerud, J. & Svendsen, J. 2016: The Last Eurasian Ice Sheets – a chronological database and time-slice reconstruction, DATED-1. *Boreas 45*, 1–45.
Ignatius, H., Axberg, S., Niemistö, L. & Winterhalter, B. 1981: Quaternary geology of the Baltic Sea. *In* Voipio, A. (ed.): *The Baltic Sea*, 54–104. Elsevier, Amsterdam.
Johansson, P., Lunkka, J. P. & Sarala, P. 2011: The glaciation of Finland. *In* Ehlers, J., Gibbard, P. L. & Hughes, P. D. (eds.): *Quaternary Glaciations – Extent and Chronology, A Closer Look*, 105–116. *Developments in Quaternary Science 15*. Elsevier, Amsterdam.
Johnsen, T. F. 2010: *Late Quaternary ice sheet history and dynamics in central and southern Scandinavia*. Ph.D. thesis, Stockholm University, 32 pp.
Kesola, R. 1985: *Bedrock map of Oulujoki area. Geological map of Finland 1:100 000, sheet 3422*. Geological Survey of Finland, Espoo.
Korpela, K. 1969: Die Weichsel-Eiszeit und ihr Interstadial in Peräpohjola (nördliches Nordfinnland) im Licht von submoränen Sedimenten. *Annales Academiae Scientiarum Fennicae A III 99*, 1–108.
Krammer, K. & Lange-Bertalot, H. 1991a: Bacillariophyceae 2/3. Centrales, Fragilariaceae, Eunotiaceae. *In* Ettl, H. J., Gerloff, J., Heynig, H. & Mollenhauer, D. (eds.): *Süßwasserflora von Mitteleuropa*, 1–576. Gustav Fisher Verlag, Stuttgart.
Krammer, K. & Lange-Bertalot, H. 1991b: Bacillariophyceae 2/4. Achnanthaceae, Kritische Ergänzungen zu Navicula (Lineolatae) und Gomphonema. *In* Ettl, H. J., Gerloff, J., Heynig, H. & Mollenhauer, D. (eds.): *Süßwasserflora von Mitteleuropa*, 1–437. Gustav Fisher Verlag, Stuttgart.
Krammer, K. & Lange-Bertalot, H. 1997a: Bacillariophyceae. 1/2. Naviculaceae. *In* Ettl, H. J., Gerloff, J., Heynig, H. & Mollenhauer, D. (eds.): *Süßwasserflora von Mitteleuropa*, 1–876. Gustav Fisher Verlag, Jena.
Krammer, K. & Lange-Bertalot, H. 1997b: Bacillariophyceae. 2/2. Bacillariaceae, Epithemiaceae, Surirellaceae. *In* Ettl, H. J., Gerloff, J., Heynig, H. & Mollenhauer, D. (eds.): *Süßwasserflora von Mitteleuropa*, 1–610. Gustav Fisher Verlag, Jena.
Laing, T. E., Pienitz, R. & Smol, J. P. 1999: Freshwater diatom assemblages from 23 lakes located near Norilsk, Siberia: a comparison with assemblages from other circumpolar treeline regions. *Diatom Research 14*, 285–305.
Lisiecki, L. E. & Raymo, M. E. 2005: A Pliocene-Pleistocene stack of 57 globally distributed benthic δ18O records. *Paleoceanography 20*, PA1003, https://doi.org/10.1029/2004PA001071.
Lotter, A. F. & Biegler, C. 2000: Do diatoms in the Swiss Alps reflect the length of ice-cover? *Aquatic Sciences 62*, 125–141.
Lundqvist, J. 1971: The interglacial deposit at Leveäniemi mine, Svappavaara, Swedish Lapland. *Sveriges Geologiska Undersökning C 658*, 163 pp.
Lunkka, J. P., Johansson, P., Saarnisto, M. & Sallasmaa, O. 2004: Glaciation of Finland. *In* Ehlers, J. & Gibbard, P. L. (eds.): *Quaternary Glaciations: Extent and Chronology. Part 1: Europe*, 93–100. *Developments in Quaternary Science 2*. Elsevier, Amsterdam.
Lunkka, J. P., Kaparulina, E., Putkinen, N. & Saarnisto, M. 2018: Late Pleistocene palaeoenvironments and the last deglaciation on the Kola Peninsula, Russia. *Arktos – the Journal of Arctic. Geosciences 4*, 1–18. https://doi.org/10.1007/s41063-018-0053-z.
Lunkka, J. P., Lintinen, P., Nenonen, K. & Huhta, P. 2016: Stratigraphy of the Koivusaarenneva exposure and its correlation across central Ostrobothnia, Finland. *Bulletin of the Geological Society of Finland 88*, 53–67.
Lunkka, J. P., Murray, A. & Korpela, K. 2008: Weichselian sediment succession at Ruunaa, Finland, indicating a Mid-Weichselian ice-free interval in eastern Fennoscandia. *Boreas 37*, 234–244.
Lunkka, J. P., Peuraniemi, V. & Nikarmaa, T. 2013: Application of till geochemical and indicator mineral data to the interpretation of the thick till sequence at Muhos, northern Finland. *Geochemistry: Exploration, Environment, Analysis 13*, 183–193.
Lunkka, J. P., Sarala, P. & Gibbard, P. 2014: The Rautuvaara section, western Finnish Lapland, revisited – new age constraints indicate a complex Scandinavian Ice Sheet history in northern Fennoscandia during the Weichselian Stage. *Boreas 44*, 68–80.
Mäkelä, E. M. 1996: Size distinction between *Betula* pollen types – a review. *Grana 35*, 248–256.
Mäkinen, K. 2005: Dating the Weichselian deposits of southwestern Finnish Lapland. *Geological Survey of Finland, Special Paper 40*, 67–78.
McQuoid, M. R. & Hobson, L. A. 1996: Diatom resting stages. *Journal of Phycology 32*, 889–902.
Mölder, K. & Tynni, R. 1967: Über Finnlands rezente und subfossile Diatomeen, I. *Comptes Rendus de la Société géologique de Finlande 39*, 199–217.

Mölder, K. & Tynni, R. 1968: Über Finnlands rezente und subfossile Diatomeen, II. *Bulletin of the Geological Society of Finland 40*, 151–170.

Mölder, K. & Tynni, R. 1973: Über Finnlands rezente und subfossile Diatomeen, VII. *Bulletin of the Geological Society of Finland 45*, 159–179.

Moore, P. D., Webb, J. A. & Collinson, M. E. 1991: *Pollen Analysis*. 216 pp. Blackwell Science, London.

Murray, A. S. & Wintle, A. G. 2000: Luminescence dating of quartz using an improved single-aliquot regenerative-dose protocol. *Radiation Measurements 32*, 57–73.

Murray, A. S. & Wintle, A. G. 2003: The single aliquot regenerative dose protocol: potential for improvements in reliability. *Radiation Measurements 37*, 377–381.

Murray, A. S., Marten, R., Johnston, A. & Martin, P. 1987: Analysis for naturally occurring radionuclides at environmental concentrations by gamma spectrometry. *Journal of Radioanalytical and Nuclear Chemistry 115*, 263–288.

Nenonen, K. 1995: *Pleistocene Stratigraphy and Reference Sections in Southern and Western Finland*. 94 pp. Geological Survey of Finland, Regional Office for Mid-Finland.

Nenonen, K., Eriksson, B. & Grönlund, T. 1991: The till stratigraphy of Ostrobothnia, western Finland, with reference to new Eemian interglacial sites. *Striae 34*, 65–76.

Niemelä, J. & Tynni, R. 1979: Interglacial and interstadial sediments in the Pohjanmaa region, Finland. *Bulletin of the Geological Survey of Finland 302*, 48 pp.

Ojala, A. E. K., Palmu, J. P., Åberg, S. & Åberg, A. 2013: Ancient shoreline database – examples of applications. *Geologi 6*, 164–173 (in Finnish).

Olley, J. M., Murray, A. S. & Roberts, R. G. 1996: The effects of disequilibria in the uranium and thorium decay chains on burial dose rates in fluvial sediments. *Quaternary Science Reviews 15*, 751–760.

Olsen, L., Sveian, H., Bergstrøm, B., Ottesen, D. & Rise, L. 2013: Quaternary glaciations and their variations in Norway and on the Norwegian continental shelf. *Geological Survey of Norway Special Publication 13*, 27–78.

Pasanen, A. & Lunkka, J. P. 2008: Glaciotectonic deformation of till covered glaciofluvial deposits in Oulu region, Finland. *Bulletin of the Geological Society of Finland 80*, 89–103.

Peltoniemi, H., Eriksson, B., Grönlund, T. & Saarnisto, M. 1989: Marjamurto, an interstadial site in a till covered esker area of central Ostrobothnia, western Finland. *Bulletin of the Geological Society of Finland 61*, 209–237.

Pienitz, R., Smol, J. P. & Birks, H. J. 1995: Assessment of freshwater diatoms as quantitative indicators of past climatic change in the Yukon and Northwest Territories, Canada. *Journal of Paleolimnology 13*, 21–49.

Pitkäranta, R. 2013: Lithostratigraphy and age of pre-Late Weichselian sediments in the Suupohja area, western Finland. *Annales Universitatis Turkuensis A II 284*, 66 pp.

Prescott, J. R. & Hutton, J. T. 1994: Cosmic ray distributions to dose rates for luminescence and ESR dating: large depths and long-term variations. *Radiation Measurements 23*, 497–500.

Reille, M. 1998: *Pollen et Spores d'Europe et d'Afrique du Nord, Supplément 2*. 521 pp. Laboratoire de Botanique Historique et Palynologie, Marseille.

Reille, M. 1999: *Pollen et Spores d'Europe et d'Afrique du Nord*. 535 pp. Laboratoire de Botanique Historique et Palynologie, Marseille.

Reitsma, T. 1969: Size modification of recent pollen grains under different treatments. *Review of Palaeobotany and Palynology 9*, 175–202.

Robertsson, A.-M. 1991: The last interglacial in northernmost Sweden. *Quaternary International 10–12*, 173–181.

Round, F. E., Crawford, R. M. & Mann, D. G. 1990: *The Diatoms. Biology and Morphology of the Genera*. 747 pp. Cambridge University Press, New York.

Rühland, K., Priesnitz, A. & Smol, J. P. 2003: Paleolimnological evidence from diatoms for recent environmental changes in 50 lakes across Canadian Arctic treeline. *Arctic, Antarctic, and Alpine Research 35*, 110–123.

Saarnisto, M. & Lunkka, J. P. 2004: Climate variability during the last interglacial-glacial cycle in NW Europe. *In* Battarbee, R. W., Gasse, F. & Stickley, C. E. (eds.): *Past Climate Variability through Europe and Africa*, 443–464. *Developments in Palaeoenvironmental Research 6*.

Saarnisto, M. & Salonen, V.-P. 1995: Glacial history of Finland. *In* Ehlers, J., Kozarski, S. & Gibbard, P. (eds.): *Glacial Deposits in North-East Europe*, 3–10. A.A. Balkema, Rotterdam.

Saarnisto, M., Eriksson, B. & Hirvas, H. 1999: Tepsankumpu revisited – pollen evidence of stable Eemian climates in Finnish Lapland. *Boreas 28*, 12–22.

Salonen, V.-P., Moreau, J., Hyttinen, O. & Eskola, K. 2014: Mid-Weichselian interstadial at Kolari, western Finnish Lapland. *Boreas 43*, 627–638.

Sarala, P. 2005: Weichselian stratigraphy, geomorphology and glacial dynamics in Southern Finnish Lapland. *Bulletin of the Geological Society of Finland 77*, 71–104.

Sarala, P., Johansson, P. & Lunkka, J. P. (eds.) 2006: *Late Pleistocene Glaciogenic Deposits in the Central Part of the Scandinavian Ice Sheet: Excursion Guide, The INQUA Peribaltic Group Field Symposium in Finland, September 11.-15.2006*, 62 pp. Geological Survey of Finland, Rovaniemi.

Sarala, P., Väliranta, M., Eskola, T. & Vaikutienė, G. 2016: First physical evidence for forested environment in the Arctic during MIS 3. *Scientific Reports 6*, 29054, https://doi.org/10.1038/srep29054.

Snoeijs, P. (ed.) 1993: *Intercalibration and Distribution of Diatom Species in the Baltic Sea 1*. 129 pp. Opulus Press, Uppsala.

Snoeijs, P. & Balashova, N. (eds.) 1998: *Intercalibration and Distribution of Diatom Species in the Baltic Sea 5*. 144 pp. Opulus Press, Uppsala.

Snoeijs, P. & Kasperovičienė, J. (eds.) 1996: *Intercalibration and Distribution of Diatom Species in the Baltic Sea 4*. 126 pp. Opulus Press, Uppsala.

Snoeijs, P. & Potapova, M. (eds.) 1995: *Intercalibration and Distribution of Diatom Species in the Baltic Sea 3*. 126 pp. Opulus Press, Uppsala.

Snoeijs, P. & Vilbaste, S. (eds.) 1994: *Intercalibration and Distribution of Diatom Species in the Baltic Sea 2*. 125 pp. Opulus Press, Uppsala.

Sorvari, S., Korhola, A. & Thompson, R. 2002: Lake diatom response to recent Arctic warming in Finnish Lapland. *Global Change Biology 8*, 171–181.

Sutinen, R. 1992: Glacial deposits, their electrical properties and surveying by image interpretation and ground penetrating radar. *Bulletin of the Geological Survey of Finland 359*, 123 pp.

Svendsen, J., Alexanderson, H., Astakhov, V., Demidov, I., Dowdeswell, J., Funder, S., Gataullin, V., Henriksen, M., Hjort, C., Houmark-Nielsen, M., Hubberten, H., Ingolfsson, O., Jakobsson, M., Kjær, K., Larsen, E., Lokrantz, H., Lunkka, J., Lysså, A., Mangerud, J., Matiouchkov, A., Murray, A., Möller, P., Niessen, F., Nikolskaya, O., Polyak, L., Saarnisto, M., Siegert, C., Siegert, M., Spielhagen, R. & Stein, R. 2004: Late Quaternary ice sheet history of northern Eurasia. *Quaternary Science Reviews 23*, 1129–1271.

Tynni, R. 1975: Über Finnlands rezente und subfossile Diatomeen, VIII. *Geological Survey of Finland Bulletin 274*, 1–55.

Tynni, R. 1978: Über Finnlands rezente und subfossile Diatomeen, X. *Geological Survey of Finland Bulletin 296*, 1–55.

Tynni, R. 1980: Über Finnlands rezente und subfossile Diatomeen, XI. *Geological Survey of Finland Bulletin 312*, 1–93.

Tynni, R. & Donner, J. 1980: A microfossil and sedimentation study of the Late Precambrian formation of Hailuoto, Finland. *Geological Survey of Finland Bulletin 311*, 1–27.

Tynni, R. & Uutela, A. 1984: Microfossils from the Precambrian Muhos formation in Western Finland. *Geological Survey of Finland Bulletin 330*, 1–38.

Väliranta, M., Salonen, J. S., Heikkilä, M., Amon, L., Helmens, K., Klimaschewski, A., Kuhry, P., Kultti, S., Poska, A., Shala, S., Veski, S. & Birks, H. H. 2015: Plant macrofossil evidence for an early onset of the Holocene summer thermal maximum in northernmost Europe. *Nature Communications 6*, 6809, https://doi.org/10.1038/ncomms7809.

Wallinga, J. & Cunningham, A. C. 2015: Luminescence Dating, Uncertainties and Age Range. *In* Rink, W. & Thompson, J. (eds.): *Encyclopedia of Scientific Dating Methods*, 1–9. Springer, Dordrecht.

Wallinga, J., Murray, A. S. & Bøtter-Jensen, L. 2002: Measurement of the dose in quartz in the presence of feldspar contamination. *Radiation Protection Dosimetry 101*, 367–370.

Weckström, J., Korhola, A. & Blom, T. 1997: The relationship between diatoms and water temperature in thirty subarctic Fennoscandian lakes. *Arctic and Alpine Research 29*, 75–92.

Wintle, A. G. 1997: Luminescence dating: Laboratory procedures and protocols. *Radiation Measurements 27*, 769–817.